Russian Geology and Geophysics © 2019, V.S. Sobolev IGM, Siberian Branch of the RAS
Vol. 60, No. 1, pp. 86–96, 2019 DOI:10.15372/RGG2019006 *Geologiya i Geofizika*

Geologic and Geochemical Features of Cretaceous Ge-Bearing Lignites in the Yenisei Middle Reaches

V.I. Naidko[a, ✉], V.A. Makarov[a], D.G. Koz'min[b], A.F. Shimanskii[a], A.I. Fertikov[a]

[a] *Siberian Federal University, pr. Svobodnyi 79, Krasnoyarsk, 660041, Russia*
[b] *OOO Kas, ul. Traktovaya 1v, Berezovka, 662521, Russia*

Received 27 February 2018; received in revised form 9 Jule 2018; accepted 26 Jule 2018

Abstract—Integrated geological and geochemical studies were performed for lignite from the Yenisei middle reaches, represented by carbonized fragments of trees with high germanium contents. Geochemical characteristics of terrigenous sediments with Ge-bearing lignite are determined. The chemical and mineral compositions, textures, and structures of carbonized wood fragments were studied. Scanning of individual cross sections of lignite fragments has revealed a regular distribution of germanium and impurity elements. Consistent patterns of the formation of Ge-containing lignites have been established, as well as the processes of their posthydrothermal transformation, which led to the impoverishment of the primary contents of the valuable component and to the input of a number of impurity elements. The latter formed rims over the lignite fragments and microveinlets with sulfide mineralization. The hypothesis has been put forward that germanium mineralization formed in lignites of the Kas basin, in particular, the Serchanskoe deposit.

Keywords: lignite, germanium, deposit, geological and geochemical researches, Ge-bearing lignites

INTRODUCTION

The spectrum of applications for germanium grows increasingly wider and already includes space-based engineering, optic fiber communication lines, semiconductor detectors, infrared optics and thermal vision devices, catalysts, luminophores, medical and pharmaceutical products (Claeys and Simoen, 2007). Current germanium output in the form of polycrystalline zone-refined ingots, pellets, single crystals, lenses for IR-optics, and substrates for microelectronics is about 150 tons yearly (Podkopaev and Shimanskii, 2013).

Germanium abundance in the Earth's crust is 1.5 ppm (Yudovich and Ketris, 2003). Ge is rather common in various facies and is accumulated in commercially viable concentrations in geological formations and deposits of various origins (Höll et al., 2007; Frenzel et al., 2014).

Globally, Ge is primarily obtained as a by-product of complex processing of polymetallic, copper, tin-silver and iron oxide ores, as well as coals (Höll et al., 2007; Li et al., 2011; Frenzel et al., 2014; Dai et al., 2014, 2015; Gamov et al., 2016).

In Russia, commercially viable Ge concentrations are confirmed in coals in the Primorsky Krai, the Sakhalin, Kuznetsk and Chita coal basins, as well as ores in copper-pyrite deposits (Bykhovsky and Potanin, 2009). According to (Ozerskii and Ekhanin, 2009), the majority of Ge-bearing coal deposits were formed in the process of fading volcanic activity in depressions bound by faults. Abnormally high Ge concentrations were confirmed in coal beds at the bottom of coal-bearing troughs.

Occurrences of Ge-bearing lignites of the middle Yenisei have been revealed in course of prospecting surveys performed at different periods led by Yu.I. Gor'kii (1963), E.S. Meitov (1968), A.P. Evdokimov (2004), and D.G. Kozmin (2014). The surveys made it possible to investigate a number of deposits and ore occurrences in the basins of the Kas, Sym, Dubches, Rassokha, and Galaktionikha Rivers flowing within three adjacent geological structures, specifically the Kas, Dubches, and Baikh basins.

Ge-bearing lignites are currently considered a promising raw material for germanium production in Russia (Ekhanin, 1997; Evdokimov et al., 2004; Ozerskii and Ekhanin, 2009). Earlier studies (Ozerskii and Ekhanin, 2009) recognized Ge-bearing lignites as a proper geological-production type, which is different from Ge-bearing coals based on three key attributes as follows:

(1) Ge-bearing lignites were formed in quiet tectonic setting undisturbed by volcanic activity.

(2) Maximum Ge accumulations are concentrated in terrigenous Cretaceous deposits hosting the lignites, while superposed over Jurassic brown coals. However, for Ge-bearing coal deposits the inverse relationship is typical. In the Primorsky Krai, high Ge concentrations are localized in the near-bottom parts of Ge-bearing coal beds, rather than in the roof of beds.

✉ Corresponding author.
E-mail adress: vinaidko@mail.ru (V.I. Naidko)

(3) Lignites cannot be considered coals. These are isolated fossil wood fragments subjected to gelification and coalification buried in sandstone layers.

Ge-bearing lignites localized in Meso-Cenozoic sediments in the Kas basin have first been revealed as a result of oil prospecting efforts in the 1960s. Further prospecting and evaluation efforts in 2011–2014 identified the most promising target in terms of commercial viability, i.e., the Kas area.

The Kas area is located at the juncture of two major geostructures, i.e., the West Siberian plate and the Yenisei Ridge.

As a result of a prospecting and evaluation campaign performed by OOO Kas in the Kas area, the Serchanskoe Ge deposit was revealed, C_1- and C_2-category reserves, as well as P_1-category inferred resources were calculated. The total P_2-category resource potential of the Ge-bearing area is 1112 tons of Ge (Makarov et al., 2014).

Aside from the Serchanskoe deposit, about 30 lignite-bearing occurrences are revealed in the Cretaceous sediments in the Kas basin (Evdokimov et al., 2004), and their closer investigation increases the possibility of discovering commercially viable Ge deposits and also raises the question of identifying a proper Ge-bearing lignite province within the studied area, which in turn defines the topicality of the research performed.

The goal of this paper is to reveal common patterns in germanium mineralization development based on studying geological and geochemical features of lignites of the middle Yenisei and terrigenous host rocks.

METODS

Geological and geochemical studies of lignites and host rocks were performed in the Serchanskoe deposit within the

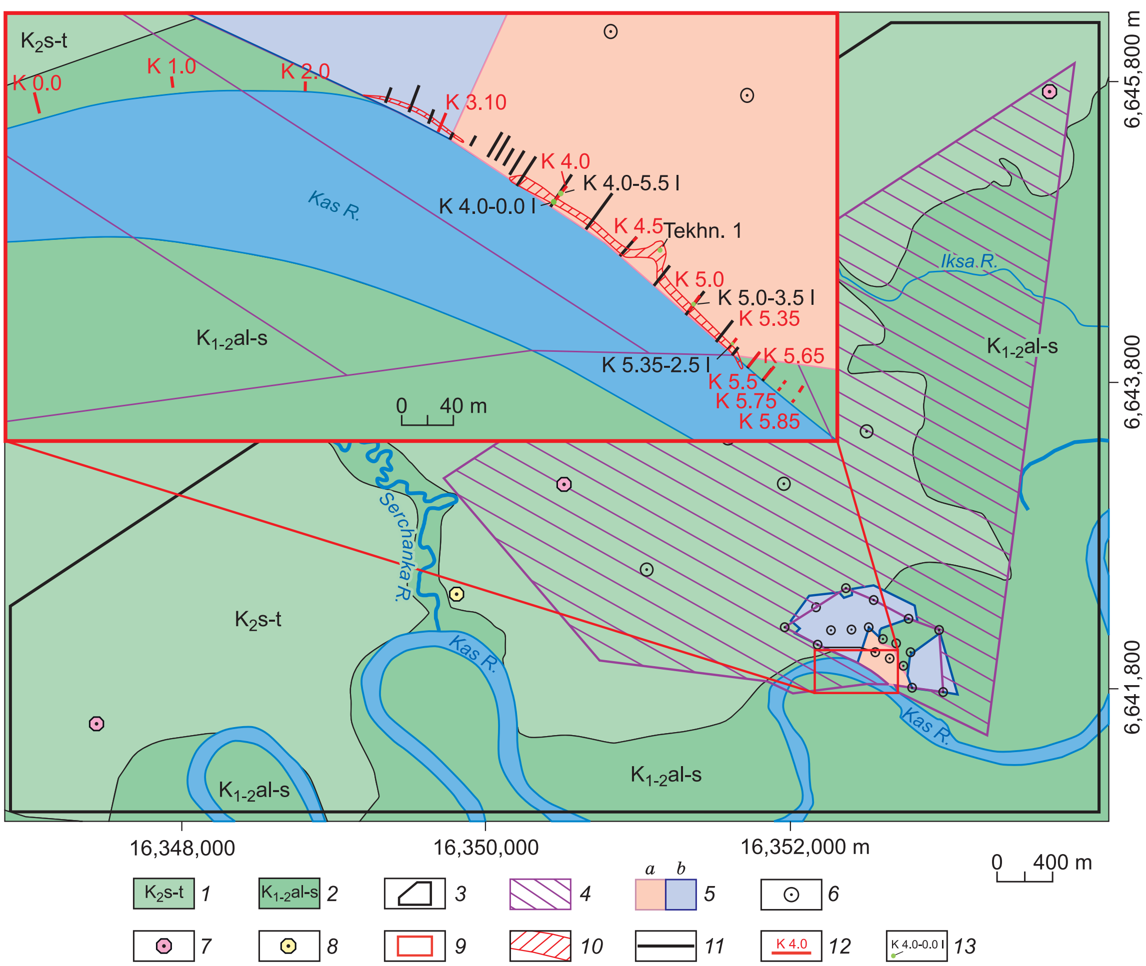

Fig. 1. Diagram of the geological structure of the Serchanskoe Ge-bearing lignite deposit (composed using archive material and modified by the authors). *1*, Upper Cretaceous, Cenomanian–Turonian stages, Simonov Formation, top layer, lacustrine-alluvial deposits, quartz sands with poorly lithified sandstone interbeds; *2*, Lower–Upper Cretaceous, Albian–Cenomanian stages, Simonov Formation, middle layer, poorly lithified gray sands with clay, siltstone and argillite interbeds; *3*, Serchanskoe deposit outline; *4*, outline of P_1-category inferred Ge resources; *5*, outlines of calculated Ge reserves: C_1-category (*a*), C_2-category (*b*); *6*, wells drilled during the prospecting and evaluation campaign of 2011–2014; *7*, wells drilled in 2003; *8*, wells drilled during oil and gas prospecting; *9*, outline of the studied area; *10*, ore body outcrop at the surface; *11*, mine workings performed in 2011–2014; *12*, mine workings smoothed and tested during the authors' field research in 2016 with numbers; *13*, lignite sample collection points.

productive interval penetrated by mine workings. Trenches in bedrock outcrops were used to collect 176 ore-bearing interval and host rock samples at an interval of 0.5 m for geochemical, mineralogical, and petrographic research. To study the material composition and mineralogical and geochemical properties, 20 lignite samples were collected. In addition, ore from large-volume technological samples and reference sample collections of AO Germaniy and OOO Kas were used to characterize textural and structural features and chemical composition of lignites, as well as ash produced as a result of their combustion.

Analytical, mineralogical, and petrographic research were performed at laboratory facilities of OOO CGI Prognoz, AO Germaniy and at the common use center of the Siberian Federal University (Krasnoyarsk).

The chemical composition of host rocks, lignites, and ash were investigated using *X-ray fluorescence* (MobiLAB X-50, XRF1800 Shimadzu spectrometer) and *atomic emission with inductively coupled plasma* (iCAP 6300 Duo Thermo Fisher Scientific). Statistical processing of the results was performed using Microsoft Excel and Statistica 8.0 software suites.

Chemical and mineral composition of ash was studied using 63 samples. As opposed to the standard technique (GOST…, 2006), lignite combustion was performed in two stages at temperatures of 350 and 550 °C with isothermal exposure of two hours at each stage aimed to avoid active lignite combustion at the initial stage and prevent volatile components from escaping.

Mineral composition of ash samples was studied using *X-ray phase* analysis (Shimadzu XRD-6000 diffractometer).

Lignite sample microstructure was studied by optical (Axioscope 40 APol) and electron (HitachiTM-3000 and JEOLJSM 7001F) microscopy.

Distribution of chemical elements in samples of carbonized wood fragments was studied by scanning X-ray fluorescence spectrometer Itrax Multi Scanner (Biogeochemistry of Ecosystems Laboratory, Siberian Federal University), using the approach described in (Fors et al., 2015). The total of 15 lignite samples of various morphologies and sizes extracted from different carbonized wood fragments (tree trunks and branches) were scanned.

RESULTS

Based on the results of field observations and mineralogical and petrographic research, it was found that the terrigenous rock section of the thoroughly studied Serchanskoe deposit area (Fig. 1) is composed bottom-up by carbonaceous mudstones, poorly lithified sandstones, and sands (Fig. 2).

Carbonaceous mudstones form the bottom part of the studied lithological section and are dark gray with intense

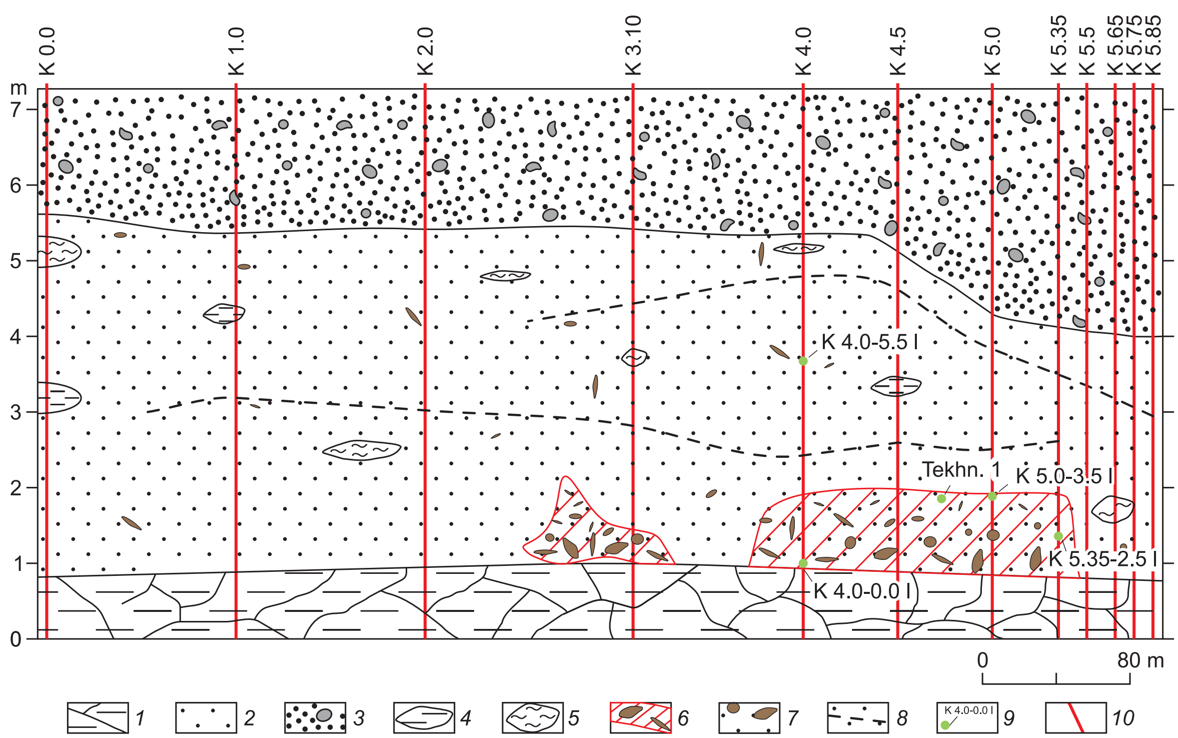

Fig. 2. Diagram of the geological section of the studied area of the Serchanskoe deposit shown in Fig. 1. *1*, carbonaceous argillites; *2*, poorly lithified sandstones; *3*, sands with pebble inclusions; *4*, argillite fragments; *5*, flattened isometric clay inclusions; *6*, outlines of ore bodies based on the prospecting and evaluation campaign of 2011–2014; *7*, isolated inclusions of lignite fragments in poorly lithified sandstones; *8*, vegetable detritus interbeds; *9*, lignite sample collection points; *10*, mine working lines drilled during the authors' field research in 2016. Numbers of mine workings are shown at the top of the figure horizontally.

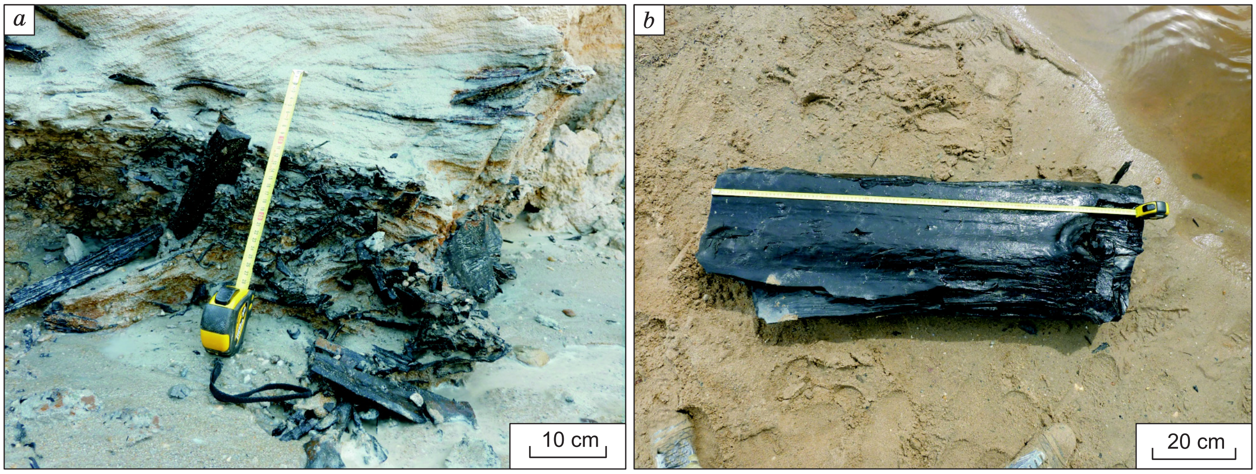

Fig. 3. Fragments of Ge-bearing lignites in poorly lithified sandstones of the Serchanskoe deposit. *a*, Small and large; *b*, major.

fractures. The visible thickness of carbonaceous mudstones is on average 1.0 m.

The middle part of the section is formed by poorly lithified sandstones, i.e., by a lignite-bearing interval that hosts ore bodies. Sandstones primarily consist of quartz and feldspar and are characterized by increased clay mineral content (kaolinite and montmorillonite). Heavy-fraction minerals are represented by pseudorutile, monacite, ilmenite, zircon, and garnet. These minerals are usually characterized by medium or poor roundness. Individual grains are light gray with fine- or medium-grain structure and are characterized by cross-bedding. The poorly lithified sandstone layer has rare inclusions of dark gray clays of flattened isometric shape, mudstone fragments sized 2 to 10 cm, thin vegetable detritus interbeds with thicknesses up to 2 mm, and occasional lignite fragments. The sandstone layer's thickness in the studied area varies from 3.0 to 5.5 m.

The sandstone layer is overlain by poorly sorted light gray or light yellow sands. The sands consist of quartz and feldspar with micaceous and clayey impurities. The sand layer includes rounded pebbles sized 1 to 3 cm represented by a wide variety of metamorphic and igneous rocks. The visible thickness of sands is on average 2 m.

Sedimentary rocks often include iron hydroxides manifested in the form of thin films in carbonaceous mudstones, as well as isometric interbeds and inclusions in lignite-bearing sandstones and overlaying sands.

Ore bodies in the deposit are visually identifiable and are represented by fragments of poorly lithified consertal sandstone layer with maximum presence of lignite fragments. The total of six bed-like ore bodies are identified in the deposit with thicknesses varying between 0.3 and 2.6 m, the average being 0.8 m. Ore bodies are traced along the strike by wells over 170 m. The intervals between ore bodies in the section reach 16 m on average as they vary from 2 to 33 m (Makarov et al., 2014).

Sandstones within the outlines of ore bodies are characterized by a highly irregular presence of lignite fragments. The lignite-bearing capacity throughout the section and along the strike ranges from 1 to 60.1%, the average being 9.6%. Lignite fragments in ore bodies occur chaotically without a common orientation. Fragments in the section of ore bodies and

Table 1. Average chemical composition of lignite based on the analysis of 63 samples, wt.%

Element	Average content	Element	Average content
Ge	0.020 ± 0.001	K	0.10 ± 0.05
C	68.0 ± 1.0	Ti	0.1 ± 0.05
O	25.0 ± 0.5	Na	<0.02
H	5.3 ± 0.5	Cr	<0.02
S	1.60 ± 0.05	Mg	<0.02
Si	1.00 ± 0.05	V	<0.01
N	0.70 ± 0.05	Co	<0.01
Al	0.50 ± 0.05		
Fe	0.4 ± 0.1	Ce, La, Nd, Sc, Y	≤0.02
Ca	0.10 ± 0.05		

Note. Concentrations are determined using ISP-MS technique at the laboratory of AO Germanii.

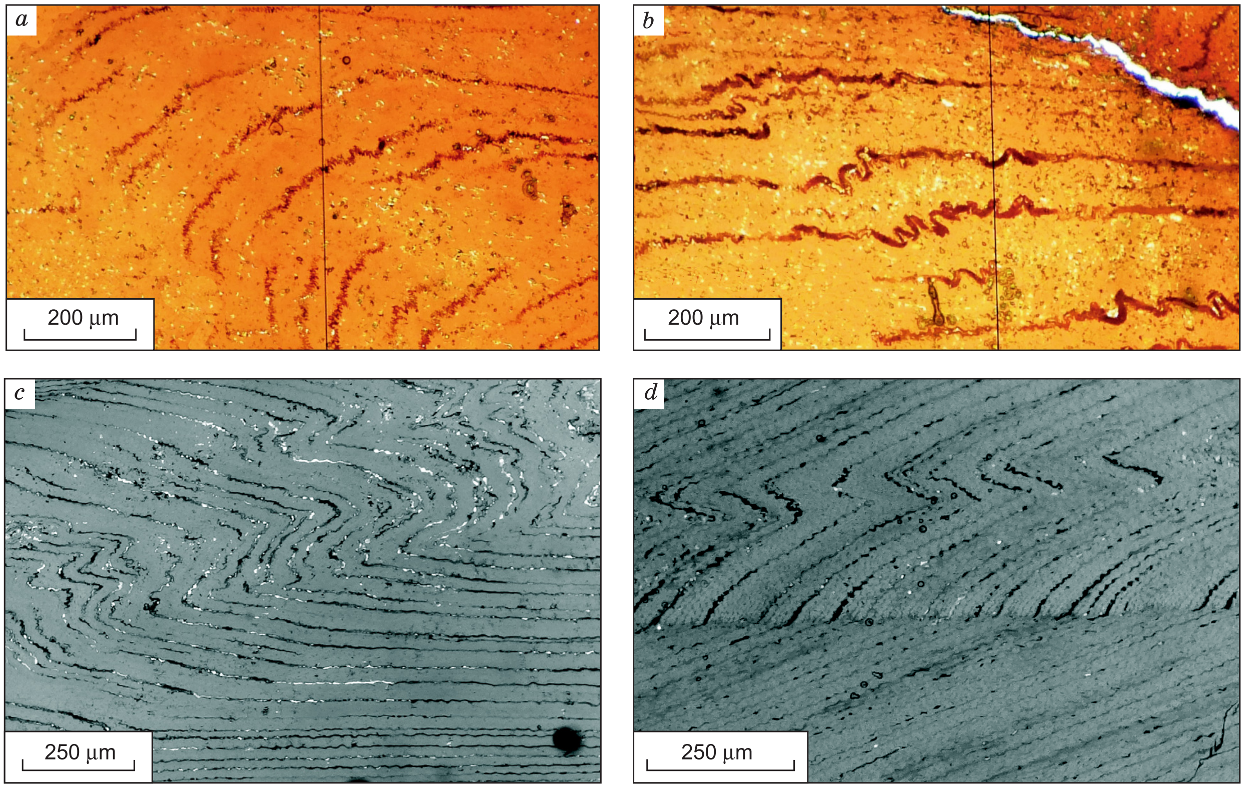

Fig. 4. Photomicrographs of lignite samples in transmitted light. *a*, Wave-like shapes of cellular fabric structure; *b*, saw tooth structure of individual cellular fibers; *c*, microfolding; *d*, cellular structure compaction zone further shifting against the outline of annual rings.

poorly lithified sandstones hosting them show a poorly sorted distribution, with smaller differences primarily concentrated in the roof.

Lignite fragments range in size from few centimeters to 1.5 m (Fig. 3). Organic matter has a pronounced wood texture. Lignites are brittle with conchoidal and occasionally splintery fractures in the cross-section. Some fragments have iron hydroxide films at their surfaces. The presence of sulfide mineralization represented by pyrite aggregates is established in shrinkage fractures. Average chemical composition of lignite fragments is presented in Table 1.

Germanium concentration in lignite fragments varies from 40 to 600 ppm. The typical composition is as follows: ~68.4 wt.% carbon, ~5.3 wt.% hydrogen, ~1.6 wt.% sulfur,

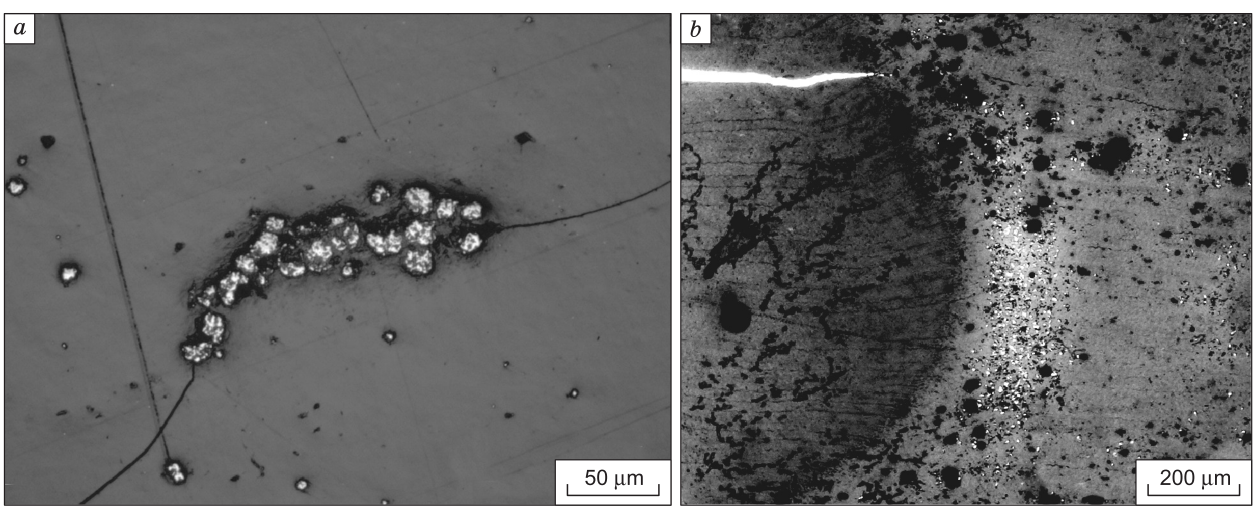

Fig. 5. Framboidal pyrite in lignite samples in reflected (*a*) and transmitted light (*b*). *a*, Individual framboidal pyrite inclusions (white) and its aggregates; *b*, pyrite mineralization in lignite cellular structure.

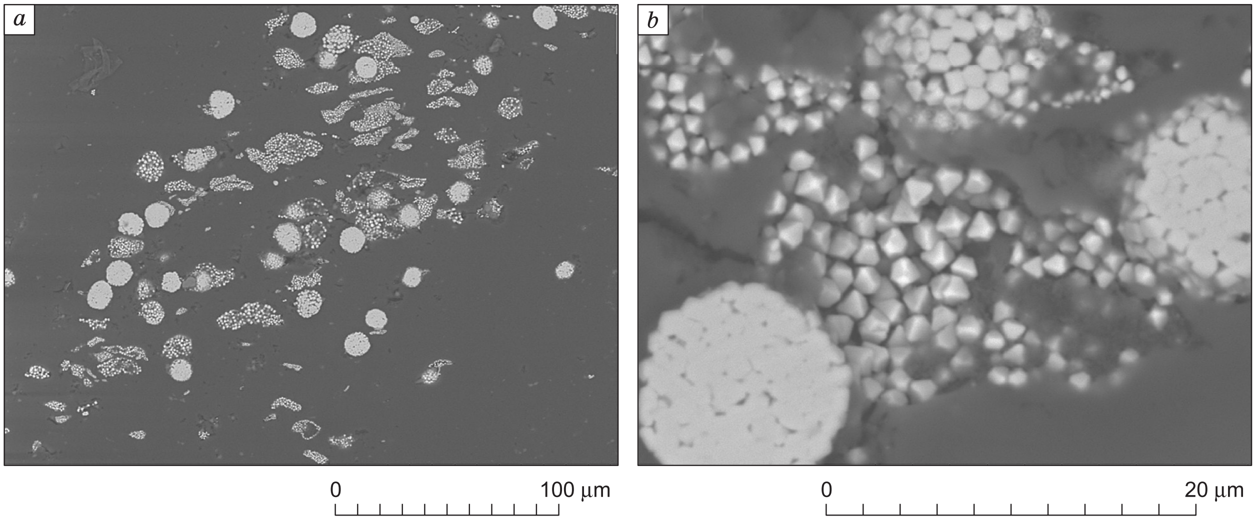

Fig. 6. Distribution of framboidal pyrite aggregates in lignite (*a*); pyrite crystals and their aggregates forming individual framboids (*b*).

~0.7 wt.% nitrogen, and ~25.0 wt.% oxygen. The prevalent metallic elements (wt.%) are silicon (~1.0), aluminum (~0.5), and iron (~0.4).

The total content of Ce, La, Nd, Sc, and Y in lignites reaches 0.02 wt.%, which makes it possible to use them as a raw material for obtaining rare earth metals (Podkopaev et al., 2016).

The results of microscopic studies of lignite samples are presented in Figs. 4–6.

In most samples, microscopy reveals the wave-like structure of dense matter in annual rings (Fig. 4*a*), as well as sawtooth shape of individual cellular fibers (Fig. 4*b*). Deformation of annual rings may be observed in the form of microfolding (Fig. 4*c*), as well as compression and shear zones (Fig. 4*d*). Certain lignite samples include cataclasis and shrinkage fractures. The textural and structural features observed indicate a postsedimentation transformation of lignites, i.e., their deformation during the diagenesis of poorly lithified sandstones that host them.

Sulfide mineralization in the studied lignite samples is confined to edges of carbonized wood fragments. Sulfides are represented by framboidal pyrite inclusions or its aggregates (Fig. 5*a*). Framboid sizes reach 10–30 µm in diameter. Pyrite is localized at the edges of cellular fibers (Fig. 5*b*), as well as shrinkage fractures (Fig. 5*a*). Octahedral and pentagondodecahedral habits of pyrite crystals forming individual framboids were observed with magnification of 5000× (Fig. 6).

Element distribution in individual carbonized wood fragments was studied using the technique and equipment applied in dendrochronology to study annual rings in trees (Fors et al., 2015).

The scanning made it possible to identify a nonuniform Ge distribution typical for all samples. Increased Ge content was revealed in the central parts of fragments. Maximum concentrations of titanium, iron, silicon, potassium, and calcium were peculiar for edges of carbonized wood fragments. All these elements define the basic material composition of lignite ash residue. Distribution pattern of Ge and other impurity elements typical for all samples is presented in Fig. 7.

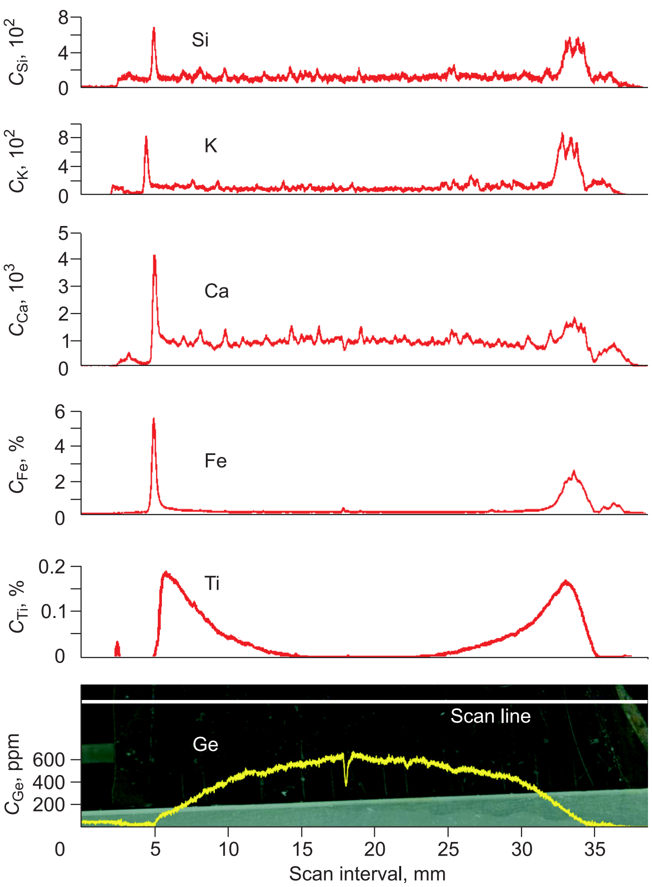

Fig. 7. Distribution of Ge and other impurity elements in the cross-section of a large (140 × 55 mm) integral lignite fragment.

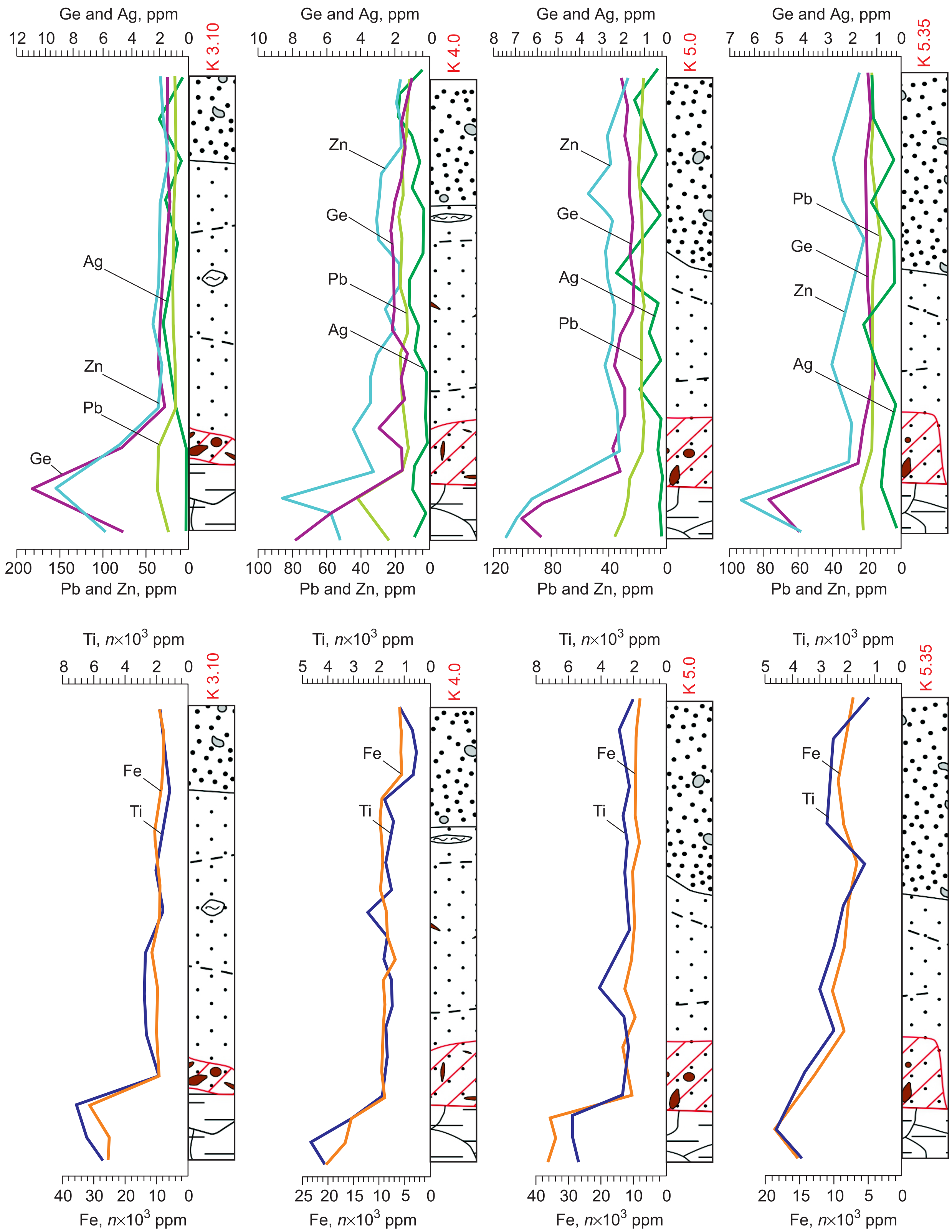

Fig. 8. Distribution diagrams for germanium, silver, titanium, and iron in the sedimentary section of the studied area of the Serchanskoe deposit. Numbers of trenches, whose locations are shown in Fig. 2, are indicated at the top of the columns.

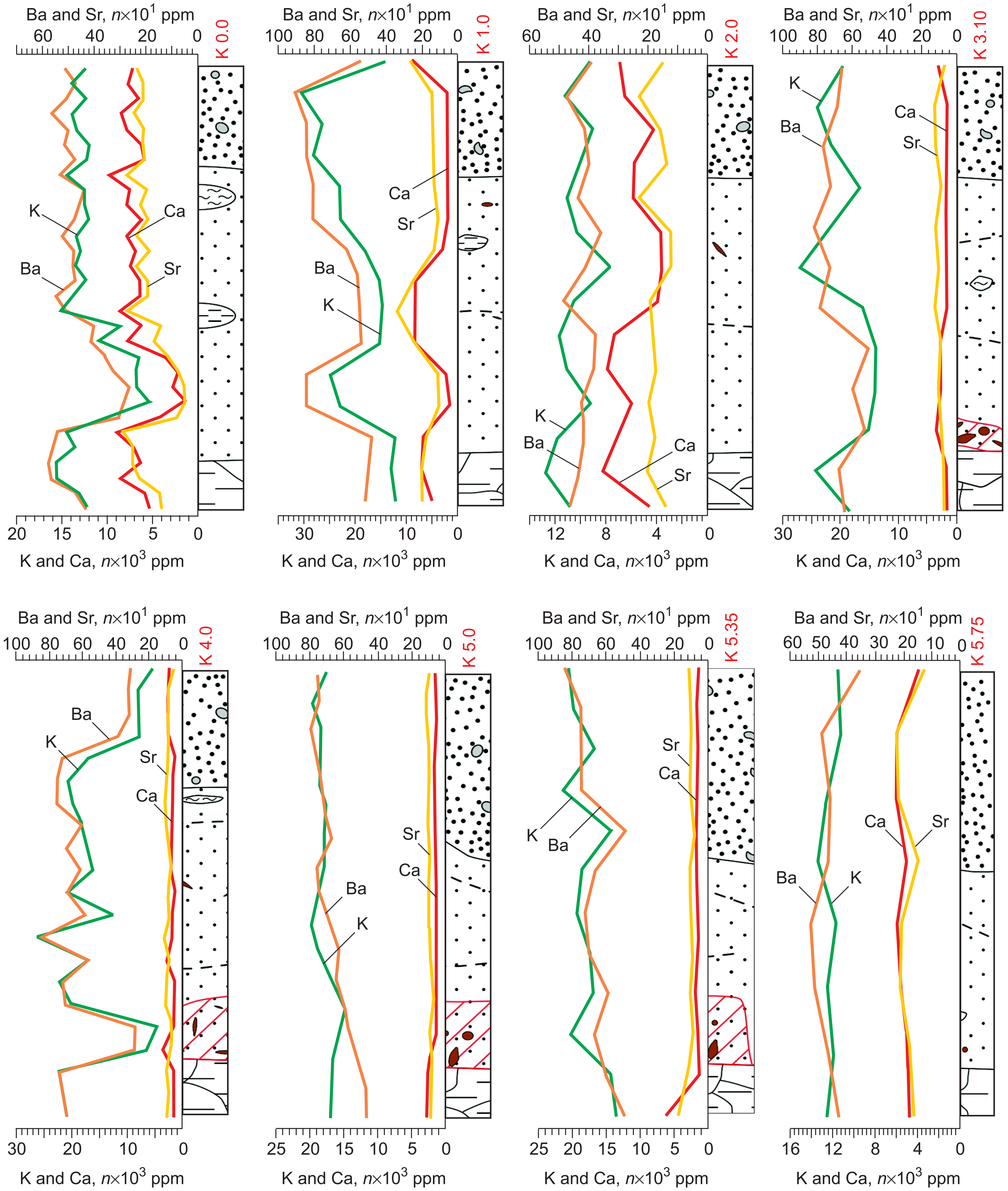

Fig. 9. Distribution diagrams for potassium, calcium, barium, and strontium in the sedimentary section of the studied area of the Serchanskoe deposit. Numbers of trenches, whose locations are shown in Fig. 2, are indicated at the top of the columns.

The scanned sample shown in Fig. 7 represents a cross-section of a large flattened lignite fragment sized 140 × 55 mm. The wood texture of organic matter was well preserved. Outlines of annual rings could be clearly seen. The thickness of dense matter between annual rings varied from 3 to 5 mm. Thin iron hydroxide films are present at the surface of the studied sample. No mineral inclusions were observed. The scanning line was transverse to the concentric-zonal wood structure of lignite.

Chemical and phase compositions of lignite combustion ash were studied. It was found that lignite ash content varies within the wide range from 1.5 to 70.0%. Lignite combus-

Table 2. Macro- and microelement composition of terrigenous deposits for the studied area of Serchanskoe deposit

Element	Sand (74 samples)	Poorly lithified sandstones—ore-bearing interval (82 samples)	Carbonaceous argillites (20 samples)
	Average content, wt.% × 10^{-2}		
Ge	0.019 ± 0.005	0.021 ± 0.009	0.042 ± 0.022
Pb	0.14 ± 0.02	0.15 ± 0.02	0.20 ± 0.08
Zn	0.30 ± 0.09	0.33 ± 0.12	0.6 ± 0.4
Fe	109.4 ± 45.3	112.1 ± 47.5	198.3 ± 93.7
Cu	0.50 ± 0.03	0.50 ± 0.04	0.6 ± 0.2
K	117.2 ± 38.5	153.2 ± 56.7	134.9 ± 25.9
Ca	44.9 ± 21.2	37.0 ± 22.5	48.9 ± 23.5
Rb	0.50 ± 0.16	0.7 ± 0.2	0.6 ± 0.2
Sr	1.5 ± 0.6	1.3 ± 0.5	1.5 ± 0.7
Zr	1.7 ± 0.8	1.7 ± 0.8	2.1 ± 0.9
Ba	4.6 ± 1.2	5.7 ± 1.6	5.0 ± 0.7
Ag	0.007 ± 0.01	0.007 ± 0.01	0.007 ± 0.01
Ti	21.6 ± 9.8	23.2 ± 9.7	37.9 ± 17.9

Note. Concentrations are determined using X-ray fluorescence method at the laboratory of OOO CGI Prognoz.

tion ash primarily includes silicon (up to 26.0 wt.%), aluminum (~9.0 wt.%), iron (~6.0 wt.%), calcium (up to 10.0 wt.%), and potassium (~1.5 wt.%). Ge concentration in the ash varies from 500 to 2500 ppm.

The following phases were discovered in the ash: SiO_2 quartz (up to 38.0 wt.%), SiO_2 cristobalite (up to 6.0 wt.%), calcium sulfate (~6.0 wt.%), Fe_2O_3 hematite (up to 8.0 wt.%), K_2SO_4 potassium sulfate (2.0 wt.%), TiO_2 rutile (~2.0 wt.%), $CaTiO_3$ perovskite (~ 1.7 wt.%), $KAlSi_3O_8$ orthoclase (up to 10.0 wt.%), and germanium oxide (up to 0.5 wt.%).

The macro- and microelement composition of terrigenous rocks in the thoroughly studied area of the Serchanskoe deposit is presented in Table 2.

Maximum concentrations of Ge and other impurity elements, such as lead, zinc, iron, copper, zircon, and titanium are associated with carbonaceous mudstones. Contents of these elements decrease towards the top of the section, with the respective concentrations reaching their minimums in sands overlaying lignite-bearing sandstones.

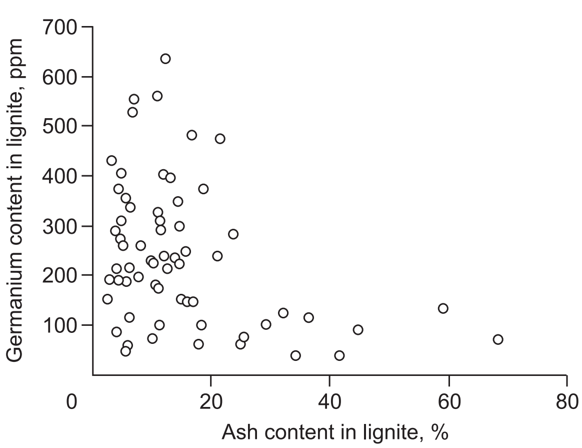

Fig. 10. Dependence between Ge content in lignite and its ash content (n = 63).

The distribution of Ge and other impurity elements across the section and along the strike of the ore-bearing interval and its host rocks is shown in Figs. 8 and 9.

The plots show significant variations in the distribution of Ge and other impurity elements across the section and along the strike of the ore-bearing interval, whereas the material composition remains relatively homogenous. This may be associated with sedimentary rock transformations in the process of hypergenic metasomatism in the Serchanskoe deposit.

DISCUSSION

Ge distribution revealed in carbonized wood fragments (Fig. 7) with maximum concentrations in their central parts probably indicates the sorption mechanism of Ge accumulation in lignite. Reduced Ge content on the periphery of fragments accompanied by increased concentrations of elements, such as titanium, iron, silicon, calcium, and potassium may indicate a change in geochemical settings, which caused intensified activity of mineralized solutions in the ore-bearing terrigenous deposits. As a result, Ge was removed from the surface layer of carbonized wood fragments, while Fe, K, Si, Ca, and possibly Ti, were brought in and formed rims at the edges of lignite fragments. Increased content of these impurity elements is likely to be the cause of increased lignite ash content. Currently, the problem of composition and genesis of hydrothermal mineralized solutions is not fully resolved and requires a detailed research.

To verify the suggested Ge sorption mechanism in carbonized wood fragments, ash residue from their combustion was studied.

Figure 10 shows the plot reflecting the relationship between Ge content in lignite and its ash content.

It was found that Ge content in low-ash (0–20%) lignites varies significantly from low (40 ppm) to high (650 ppm). Ge content in high-ash (20–70%) lignites also varies, but in the lower value range (50 ppm). Increased Ge concentrations in low-ash lignites indicate that Ge content is related to the organic matter, which in turn confirms the conclusions made on the sorption mechanism of Ge ore formation in carbonized wood with further impoverishment of initial Ge concentrations due to mineralized hydrothermal solution activity, which then leads to increased lignite ash content.

Pyrite mineralization of clear authigenic origin was formed during the hydrothermal transformation of lignites in cavities and decompaction zones. This, in turn, confirms the hypothesis on secondary changes in carbonized wood fragments in the process of hypergenic metasomatism occurring in poorly lithified sandstones that host Ge-bearing lignites.

Geochemical studies of ore-bearing deposits revealed specific features in the distribution of chemical elements, which indicate that secondary hydrothermal transformations took place in the thoroughly studied sedimentary section of the Serchanskoe deposit.

It was found that Ge and impurity elements, namely Pb, Zn, Fe, Cu, and Ti, were distributed nonuniformly (Fig. 8). Maximum concentrations of elements were associated with carbonaceous mudstones underlying lignite-bearing sandstones. Concentrations of most elements decrease towards the top of the section, the only exceptions being lead and zinc, whose geochemical fields are similarly expressed in poorly lithified sandstones in the central part of the studied area.

Ge distribution is relatively uniform within the outlines of ore bodies and poorly lithified sandstones that host them. A slight increase in concentration is seen within the outline of the ore body at the bottom of the layer, where the maximum concentration of carbonized wood fragments is observed.

Maximum concentrations of impurity elements in carbonaceous mudstones are clearly caused by the presence of organic matter, which provides increased sorption capacity of the terrigenous interval.

The following peculiarities in distribution of elements along the strike of the ore-bearing interval are to be noted. Increased silver concentrations occur regularly throughout the whole poorly lithified sandstone layer (Fig. 8). Increased contents of zircon are also confined to sandstones, especially the bottom part of the layer.

Distributions of K, Ba, Ca, and Sr in the section and along the strike of terrigenous deposits are highly irregular (Fig. 9). Increased potassium and barium concentrations were primarily specific for the central part and partially the western flank of the studied area. At the same time, spatial correlation is the opposite for geochemical fields of calcium and strontium, i.e., their maximum concentrations are observed at the flanks of the studied area.

The discovered geochemical features of terrigenous deposits, namely the pronounced irregularity in distributions of Ge and other impurity elements across the section and along the strike of the sedimentary mass, are likely to be the indicators of hydrothermal solution activity, which manifested itself at the initial diagenesis stage. The presence of framboidal pyrite in lignite implies that transformations occurred at temperatures about 100–150 °C (Kizil'shtein, 1969; Kizil'shtein and Minaeva, 1972) under high iron-oxidizing bacteria activity. The presence of limonite films and contractions in the ore-bearing interval may also be associated with iron-oxidizing bacteria.

CONCLUSIONS

The discovered geological and geochemical features of Ge-bearing lignites allow us to conclude that they were formed in several stages that occurred in specific facial and geochemical settings.

The gently dipping layer of Cretaceous–Paleogenic clastic sediments of the Kas basin was formed at the deposition stage, where wood fragments (tree trunks, branches, etc.) were accumulated in the form of sheet deposits. The deposits were formed under humid climate favorable for vegetation of hygrophilous trees on vast areas. Accumulation of clastic rocks in lignite-bearing interval occurred in alluvial-lacustrine facies in quiet tectonic setting favorable for the formation of accumulative plains with dense river system and abundance of lakes.

The buried fragments of fossil trees were carbonized, flattened and deformed with formation of fractures and microfold structures in annual rings during sediment compaction and diagenesis. It is possible that mineralization was formed at the initial diagenesis stage as a result of wood fragments absorbing Ge from solutions that drained the lignite-bearing interval.

Ore bodies of the Yenisei Ridge could be a possible source of Ge in lignites of the Kas basin. Multiple Ge-bearing pyrite-polymetallic deposits and occurrences, which could be possible sources of rare metals, were discovered at the western slope of the ridge adjacent to the basin's deposits. These ore bodies include the unique Gorevskoe deposit with increased Ge concentrations in the ore from 18 to 159 ppm, ore occurrences in the Teneginskoe ore field with Ge content of up to 200 ppm and other polymetallic deposits. The aforementioned bodies were subjected to weathering and erosion, and the ore matter was transported to deposition basins, including the Kas basin located 40–50 km to the west. Lignites were the main Ge sorbent, which provided its commercially viable concentrations.

At the final stage of Ge deposit formation, lignite transformation occurred, which manifested itself in removal of germanium from edges of carbonized wood fragments, while Si, Ca, K, Fe, and Ti were brought in thereby forming high-ash rims. Diagenetic hydrothermal transformation of lignites occurred under iron-oxidizing bacteria activity and was accompanied by sulfide mineralization represented by framboidal pyrite and limonite accumulations.

The work was supported by the Russian Foundation for Basic Research, the Government of the Krasnoyarsk Krai, the Krasnoyarsk Regional Fund for Support of Scientific and Scientific-Technical Activity, project No. 16-43-240719.

REFERENCES

Bykhovsky, L.Z., Potanin, S.D., 2009. Geology-industrial types of rare-metal deposits. Mineral Products. Geological and Economic Series, Vol. 28. VIMS, Moscow.

Claeys, C., Simoen, E., 2007. Germanium-Based Technologies: From Materials to Devices. Elsevier, Berlin.

Ekhanin, A.G., 1997. Issues of germanium-bearing potential of coals and lignites in the southern part of the Tunguska Basin, in: Raw Material Resources of the Lower Angara Region [in Russian]. Directorate of the Federal Target Program on Resource Development in Lower Angara Region in Krasnoyarsk Krai, Krasnoyarsk, pp. 49–51.

Evdokimov, A.P., Ozerskii, A.Yu., Ekhanin, A.G., 2004. Germanium-bearing lignites of the south-eastern margin of the West Siberian Plate. Razvedka i Okhrana Nedr, No. 6, 26–29.

Fors, Y., Grudd, H., Rindby, A., Bornmalm, L., 2015. X-ray fluorescence for cultural heritage: scanning biochemical fingerprints in archaeological shipwrecks. Spectrosc. Eur. 27 (1), 11–13.

Frenzel, M., Ketris, M.P., Gutzmer, J., 2014. On the geological availability of germanium. Miner. Deposita 49, 471–486.

Gamov, M.I., Levchenko, S.V., Rylov, V.G., Rybin, I.V., Trufanov, A.V., 2016. Metal-containing coals of the East-Donetsk basin: Regularities of formation and integrated-use prospects. Russian Geology and Geophysics 57 (8), 1475–1485.

GOST 11022-95, 2006. Interstate Standard. Solid Mineral Fuel. Method for Determination of Ash. [in Russian] Standartinform, Moscow.

Höll, R., Kling, M., Schroll, E., 2007. Metallogenesis of germanium—A review. Ore Geol. Rev. 30 (3–4), 145–180.

Kizil'shtein, L.Ya., 1969. On the issue of origin of framboidal pyrite forms. Izv. Akad. Nauk SSSR, Ser. Geol., No. 5, 61–68.

Kizil'shtein, L.Ya., Minaeva, L.G., 1972. Origin of framboidal pyrite forms. Dokl. Akad. Nauk SSSR 206 (5), 1187–1189.

Li, J., Zhuang, X., Querol, X., 2011. Trace element affinities in two high-Ge coals from China. Fuel 90 (1), 240–247.

Makarov, V.A., Podkopaev, O.I., Koz'min, D.G., Naidko, V.I., Shimanskii, A.F., Kopytkova, S.A., 2014. Lignite from the central watershed of the Yenisei River and prospects for their use for manufacture of germanium. Journal of Siberian Federal University. Engineering & Technologies 7 (7), 862–871.

Ozerskii, A.Yu., Ekhanin, A.G., 2009. Research and development prospects of germanium resources in lower cretaceous lignites of the Kas Area. Bulletin of the Tomsk Polytechnic University 314 (1), 41–43.

Podkopaev, O.I., Shimanskii, A.F., 2013. Growing Low-Dislocation and Low-Impurity Germanium Single Crystals [in Russian]. Siberian Federal University, Krasnoyarsk.

Podkopaev, O.I., Balakchina, E.S., Losev, V.N., Kopytkova, S.A., Kulagin, V.A., Shimanskii, A.F., 2016. Rare earth elements in the lignite ash determination method development. Journal of Siberian Federal University. Engineering & Technologies 9 (8), 1238–1246.

Dai, S., Seredin, V.V., Ward, C.R., Jiang, J., Hower, J.C., Song, X., Jiang, Y., Wang, X., Gornostaeva, T., Li, X., Liu, H., Zhao, L., Zhao, C., 2014. Composition and modes of occurrence of minerals and elements in coal combustion products derived from high-Ge coals. Int. J. Coal Geol. 121, 79–97.

Dai, S., Liu, J., Ward, C.R., Hower, J.C., Xie, P., Jiang, Y., Hood, M.M., O'Keefe, J.M.K., Song, H., 2015. Petrological, geochemical, and mineralogical compositions of the low-Ge coals from the Shengli Coalfield, China: A comparative study with Ge-rich coals and a formation model for coal-hosted Ge ore deposit. Ore Geol. Rev. 71, 318–349.

Yudovich, Ya.E., Ketris, M.P., 2003. Germanium in Coals [in Russian]. Komi Scientific Center, Russian Academy of Sciences, Ural Branch, Syktyvkar.

Editorial responsibility: V.N. Sharapov